

树叶基前驱体碳热冲击制备乱层石墨烯及其结构演化研究

顾旭, 刘怡, 蔡胤劼, 高尚, 王宇轩, 邹菁云*

苏州科技大学物理科学与技术学院, 江苏 苏州

收稿日期: 2026年5月8日; 录用日期: 2026年6月2日; 发布日期: 2026年6月12日

摘要

乱层石墨烯因其层间错位与弱耦合特征而有高化学活性, 在储能、电催化及导电网络构建等领域具有良好应用前景。生物质前驱体是制备乱层石墨烯的优秀碳源, 具有含碳量高、来源广泛的优点, 但现有乱层石墨烯制备方法无法有效将生物质前驱体转化为乱层石墨烯。本文采用碳热冲击技术, 利用其毫秒级快速升降温的瞬态热冲击特性, 以树叶为前驱体快速制备乱层石墨烯, 并研究冲击功率与脉冲频率对产物结构演化的影响。适中的冲击功率有利于降低产物缺陷并提高结晶度, 高脉冲频率则有利于减少片层层数。本文为基于生物质的乱层石墨烯的制备提供了新思路, 为后续其的大规模可控制备提供了参考。

关键词

碳热冲击, 乱层石墨烯, 树叶, 结构演化

Study on the Preparation of Turbostratic Graphene from Leaf-Derived Precursors by Carbon Thermal Shock and Its Structural Evolution

Xu Gu, Yi Liu, Yinjie Cai, Shang Gao, Yuxuan Wang, Jingyun Zou*

School of Physical Science and Technology, Suzhou University of Science and Technology, Suzhou Jiangsu

Received: May 8, 2026; accepted: June 2, 2026; published: June 12, 2026

Abstract

Turbostratic graphene exhibits high chemical reactivity due to its interlayer misalignment and

*通讯作者。

文章引用: 顾旭, 刘怡, 蔡胤劼, 高尚, 王宇轩, 邹菁云. 树叶基前驱体碳热冲击制备乱层石墨烯及其结构演化研究[J]. 材料科学, 2026, 16(6): 31-38. DOI: 10.12677/ms.2026.166135

weak interlayer coupling, and thus shows promising application prospects in energy storage, electrocatalysis, and conductive network construction. Biomass precursors are excellent carbon sources for the preparation of turbostratic graphene because of their high carbon content and wide availability; however, existing preparation methods for turbostratic graphene cannot efficiently convert biomass precursors into turbostratic graphene. In this work, carbon thermal shock was employed to rapidly prepare turbostratic graphene using leaves as the precursor by taking advantage of its transient thermal-shock characteristics associated with rapid heating and cooling on the millisecond timescale. The effects of shock power and pulse frequency on the structural evolution of the products were further investigated. A moderate shock power was found to be beneficial for reducing product defects and improving crystallinity, whereas a high pulse frequency was favorable for decreasing the number of graphene layers. This study provides a new approach for the preparation of biomass-based turbostratic graphene, offering a reference for its subsequent large-scale controllable preparation.

Keywords

Carbon Thermal Shock, Turbostratic Graphene, Leaves, Structural Evolution

Copyright © 2026 by author(s) and Hans Publishers Inc.

This work is licensed under the Creative Commons Attribution International License (CC BY 4.0).

<http://creativecommons.org/licenses/by/4.0/>



Open Access

1. 引言

石墨烯作为一种典型的二维碳材料,因其优异的电导率、高比表面积、良好的力学性能及化学稳定性,在储能、电催化、传感及柔性电子器件等领域展现出广阔的应用前景[1]-[4]。近年来,随着研究的不断深入,人们逐渐认识到石墨烯材料的性能不仅取决于其层数,还与层间堆垛方式及缺陷结构密切相关[5]。乱层石墨烯是由石墨烯片层错位、旋转并无序堆垛形成的弱层间耦合层状碳材料,由于其层间错位及弱耦合特征,在离子传输、电荷传导及界面反应等方面表现出更高的结构适应性,因此在电化学储能及催化领域受到广泛关注[6]-[8]。

目前,石墨烯的制备方法主要包括机械剥离法、化学气相沉积法(CVD)及氧化还原法等[3] [9]-[12]。机械剥离法虽可获得高质量单层石墨烯,但产量极低,难以实现规模化制备;CVD法可实现大面积生长,但工艺复杂且成本较高;氧化还原法虽具有一定规模化优势,但产物中通常含有较多缺陷及残余含氧官能团,难以获得结构可控的石墨烯材料[13]-[15]。因此,这些方法适用于制备规则AB堆垛的石墨烯,无法快速制备具有卷曲片层结构的乱层石墨烯[11]。

碳热冲击(Carbon Thermal Shock, CTS)是通过电流瞬态加热在毫秒级时间内将材料加热至数千开尔文,并迅速冷却,从而构建出典型的非平衡热环境的快速制备方法[16][17]。相关研究表明,碳热冲击可在短时间内驱动含碳前驱体完成脱氧、脱氢及石墨化,实现石墨烯的快速制备[18]-[20]。近年来,多项研究表明,碳热冲击可利用废橡胶、废塑料等含碳废料作为碳源,实现石墨烯的快速绿色制备[6] [21]-[24]。落叶作为一种来源广泛、成本低廉的碳源,因此极具应用潜力[24][25]。然而,与其他碳源相比,树叶等生物质材料中含有大量羟基、羧基及醚键等含氧官能团,其热转化过程涉及脱水、脱羧及碳骨架重排等多级反应[26][27]。这些反应过程与碳骨架的形成与演化相互耦合,使得最终产物的层状结构及堆垛方式更加复杂。已有研究表明,利用碳热冲击技术处理生物质前驱体,可在极短时间内实现多层石墨烯的形成,但其结构调控机理仍有待深入研究[19]。

基于此, 本文以树叶为碳源, 采用碳热冲击技术制备乱层石墨烯材料, 并从能量输入强度与时间长度两个方面说明碳源由无序结构向乱层石墨烯转变的物理机制。本研究旨在为生物质基石墨烯材料的可控制备提供理论依据, 同时为理解瞬态非平衡热条件下碳材料结构重构过程提供新的研究思路。

2. 实验部分

本实验选用杨树叶作为前驱体, 首先使用去离子水对其反复清洗以去除表面尘土和可溶性杂质, 随后置于 60℃ 鼓风干燥箱中干燥 12 h 至质量基本恒定。干燥样品经机械粉碎后过 200 目筛, 获得粒径小于 75 μm 的杨树叶粉末。制备时, 以多壁碳纳米管薄膜(厚度: 20 μm , 尺寸: 4 cm \times 3 cm, 捷迪纳米科技)作为制备载体, 并以高纯氩气(纯度: 99.999%, 圣马气体)作为保护气。表征方面, 采用红外测温计(CIT-2MK2-T0640A-HS1MS-CM0, 中科红外)监测温度变化, 采用扫描电子显微镜(SEM, Quanta 400 FEG, FEI)和透射电子显微镜(TEM, Tecnai G2 F20S-TWIN, FEI)表征产物形貌, 采用拉曼光谱仪(LabRAM HR, HORIBA Jobin Yvon)分析产物的结构缺陷, 采用 N_2 吸附-脱附测试分析产物的比表面积和孔径分布, 并分别通过 Brunauer-Emmett-Teller (BET)法和 Barrett-Joyner-Halenda (BJH)法计算比表面积及孔结构参数。

3. 结果与讨论

图 1(a)是碳热冲击制备乱层石墨烯的整体示意图, 使用碳纳米管薄膜作为载体和加热元件, 包覆清洗粉碎后的树叶粉末前驱体以进行反应(图 1(b))。实验过程中, 采用 800 W、1000 W、1200 W 和 1400 W 等不同冲击功率进行反应, 随着脉冲功率的提高, 反应区温度随之升高至 1120 K、1754 K、2253 K 和 2785 K, 前驱体由初始碳化过渡至石墨化, 最终形成乱层石墨烯(图 1(c)~(f))。图 1(g)展示了碳热冲击过程中的温度演化曲线: 体系在 190 ms 内由 300 K 快速升温至 2740 K, 平均升温速率为 1.28×10^4 K/s; 在随后的降温阶段, 体系在 470 ms 内恢复至室温, 平均降温速率为 2.77×10^3 K/s。这一结果说明碳热冲击过程具有快速升温、快速降温和短时高温维持的瞬态热响应特征。

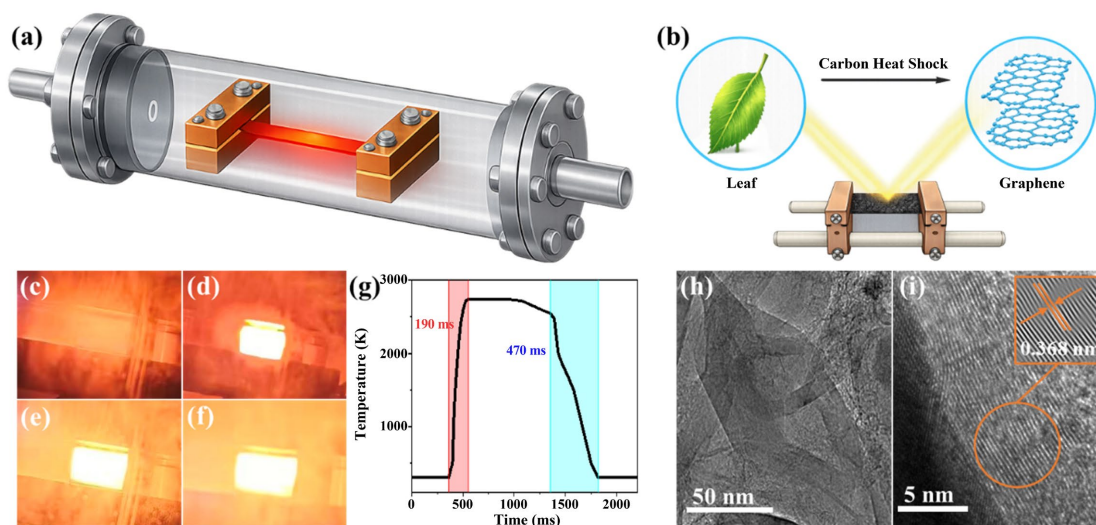


Figure 1. Carbon thermal shock technology and product characterization: (a) Schematic illustration of the apparatus; (b) Schematic illustration of the synthesis process; (c) Synthesis process at 800 W; (d) Synthesis process at 1000 W; (e) Synthesis process at 1200 W; (f) Synthesis process at 1400 W; (g) Temperature-time evolution curve during the shock process; (h) TEM image of the product; (i) HRTEM image of the product and the local lattice fringe spacing

图 1. 碳热冲击技术及其产物表征: (a) 装置示意; (b) 合成过程示意; (c) 800 W 下的合成过程; (d) 1000 W 下的合成过程; (e) 1200 W 下的合成过程; (f) 1400 W 下的合成过程; (g) 冲击过程的温度-时间演化曲线; (h) 产物的 TEM 图像; (i) 产物的 HRTEM 图像及局部晶格条纹间距

在毫秒级快速升降温所形成的瞬态热冲击作用下，树叶前驱体实现了向乱层石墨烯的快速转化。图 1(h)显示产物整体呈现出明显的薄片状形貌，片层边缘较为清晰，局部区域可观察到褶皱、卷曲及多层层交叠现象，表现出类似“纸张堆叠”的形态特征，这种褶皱结构通常源于二维碳材料在快速热应力释放及收缩过程中的形变行为，是石墨烯的重要形貌特征。图像中不同区域的明暗差异表明片层厚度并不完全一致，其中较亮区域对应较薄片层，较暗区域则反映出局部多层重叠或堆垛加厚，展现了乱层石墨烯的无序堆垛特征。图 1(i)显示，产物局部区域存在较清晰且近平行排列的层状晶格条纹，说明产物结晶度高，对局部条纹测得间距约为 0.368 nm，该数值明显大于理想石墨(002)晶面的层间距，说明产物层间堆垛方式偏离规则 AB 堆垛方式，呈现出乱层石墨烯的弱层间耦合特征。另一方面，图 1(i)中晶格条纹并非长程严格平直排列，而是表现出局部弯曲、错位及取向变化，说明其结构特征为“局部有序而整体无序”，体现了乱层石墨烯的无序堆垛特征。综合而言，所得乱层石墨烯具有高结晶度、弱层间耦合和无序堆垛的结构特性。

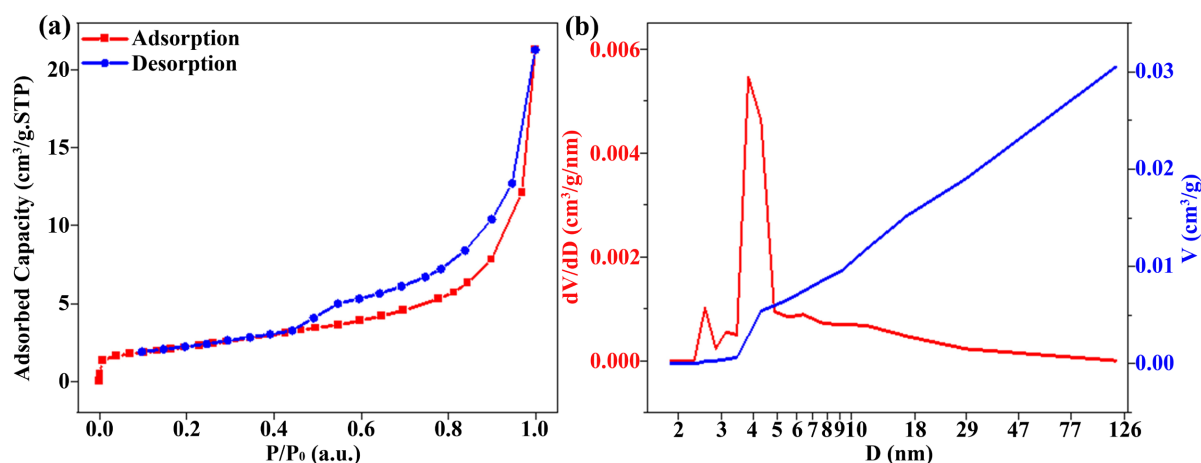


Figure 2. Pore structure characterization of turbostratic graphene: (a) N_2 adsorption-desorption isotherm; (b) Pore size distribution curve derived from the BJH desorption branch

图 2. 乱层石墨烯的孔结构表征：(a) N_2 吸附 - 脱附等温线；(b) BJH 脱附支路孔径分布曲线

Table 1. Specific surface area and pore structure parameters of turbostratic graphene

表 1. 乱层石墨烯的比表面积及孔结构参数

参数	数值	参数	数值
BET 比表面积	8.07 m^2/g	BJH 脱附平均孔径	9.75 nm
Langmuir 比表面积	12.56 m^2/g	BJH 脱附最可几孔径	3.84 nm
总孔容	0.0289 cm^3/g	BJH 吸附平均孔径	11.40 nm
BJH 脱附孔容	0.0305 cm^3/g	BJH 吸附最可几孔径	2.43 nm
BJH 吸附孔容	0.0278 cm^3/g	T-Plot 微孔比表面积	0 m^2/g
BET 平均孔径	14.32 nm	T-Plot 微孔容积	0 cm^3/g

为进一步分析所得乱层石墨烯的孔结构，对产物进行 N_2 吸附 - 脱附测试。由图 2(a)可见，产物在低相对压力区的吸附量较低，说明微孔填充作用并不明显；随着相对压力升高，吸附量逐渐增加，并在高相对压力区出现明显上升，同时吸附支路与脱附支路之间存在一定滞后现象，表明产物中存在由片层堆

叠、卷曲或局部团聚形成的介孔或大孔空隙。进一步采用 BJH 法分析孔径分布,如图 2(b)所示,脱附支路孔径分布曲线在约 3~4 nm 范围内出现明显峰值,由表 1 可知其对应最可几孔径为 3.84 nm,平均孔径为 9.75 nm,说明产物孔结构主要位于介孔范围。与此同时,T-Plot 分析结果显示产物微孔比表面积和微孔容积均接近于 0,表明所得产物并非微孔主导型多孔碳材料,其孔结构主要来源于乱层石墨烯片层之间的堆叠间隙、卷曲结构及局部团聚形成的开放孔道,处于 3~10 nm 的介孔范围。上述结果与 TEM 中观察到的片层交叠和褶皱形貌相一致,进一步说明所得乱层石墨烯存在无序堆垛的结构特性,且具有开放孔隙结构。

冲击功率决定反应区的温度,由此影响产物乱层石墨烯的缺陷水平和结晶程度。图 3(a)展示了树叶和不同冲击功率下制备的乱层石墨烯的拉曼光谱,碳热冲击后的样品均呈现明显的拉曼 D、G 和 2D 特征峰,表明树叶转化为乱层石墨烯。然而,不同功率下产物的 D、G 和 2D 特征峰的相对强度存在明显差异,进一步计算可得,其 G 峰与 D 峰的相对强度比(I_G/I_D)存在显著差异,说明其结晶程度存在差别。图 3(b)是 I_G/I_D 随冲击功率演化的规律,可以看出 I_G/I_D 随冲击功率变大呈现先升高后下降的变化趋势,说明了随着冲击功率变大,产物结晶度先升高后降低。在较低功率下,体系热输入有限,树叶前驱体虽已发生初步碳化,但脱氧、脱氢和碳原子重排仍不充分,样品中保留了较多无序碳。随着功率升高,瞬态热输入增强,前驱体热解更加充分,含氧官能团等持续脱除,碳材料 sp^2 网络逐步扩展,碳骨架有序度提高。当功率达到 1200 W 时, I_G/I_D 最高,此条件下形成了缺陷少、结晶程度高的乱层石墨烯。继续升高功率, I_G/I_D 减小,说明过高功率并未进一步改善结构,反而诱导了新的缺陷生成,因为局部温度和热应力进一步增大,片层边缘及薄弱区域更易发生断裂和局部剥离,使已形成的有序碳结构受到破坏。总结而言,功率升高一方面促进前驱体石墨化,另一方面过强的热冲击又会导致产物出现热损伤。在本实验条件下,1200 W 即为最佳冲击功率,可制得缺陷少、结构完整且结晶程度高的乱层石墨烯。

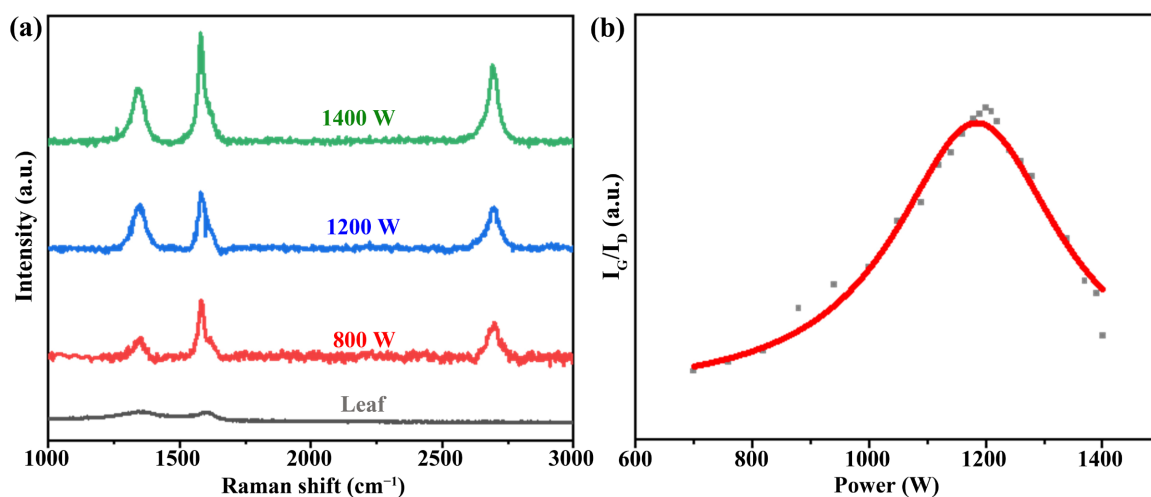


Figure 3. Raman spectra of the products at different powers and the variation of I_G/I_D : (a) Raman spectra of the leaf precursor and the products obtained at 800 W, 1200 W, and 1400 W; (b) Corresponding variation curve of I_G/I_D with shock power
图 3. 不同功率下产物的拉曼光谱及 I_G/I_D 变化情况: (a) 树叶及 800 W、1200 W、1400 W 下产物的拉曼光谱; (b) 冲击功率与 I_G/I_D 的对应变化曲线

此外,脉冲频率通过调控单次加热的时间尺度及热输入节奏,决定体系在高温区的停留时间及热循环速率,从而影响产物的整体结构。图 4(a)展示了不同脉冲频率下制备的乱层石墨烯的拉曼光谱,其 2D 峰相对强度随着频率升高而不断增大。图 4(b)是 G 峰与 2D 峰相对强度的比值(I_G/I_{2D})随脉冲频率演化的

规律,可以看出 I_G/I_{2D} 随着频率升高而不断减小,说明了所得乱层石墨烯的层数随着频率的升高而减少。这是因为频率的升高会缩短单次加热与冷却过程的持续时间,使已石墨化的片层经历更频繁的热胀冷缩,从而削弱层间范德华相互作用并促进片层剥离,最终得到层数更少的乱层石墨烯。另一方面,高脉冲频率也会导致前驱体中环氧基和羟基分解产生的气体快速膨胀,令石墨烯层间压力增大至打破维系层间堆叠的范德华相互作用,使得所得乱层石墨烯的层数减少[28][29]。总结而言,提高脉冲频率能制得层数更少、层间耦合更弱的乱层石墨烯。

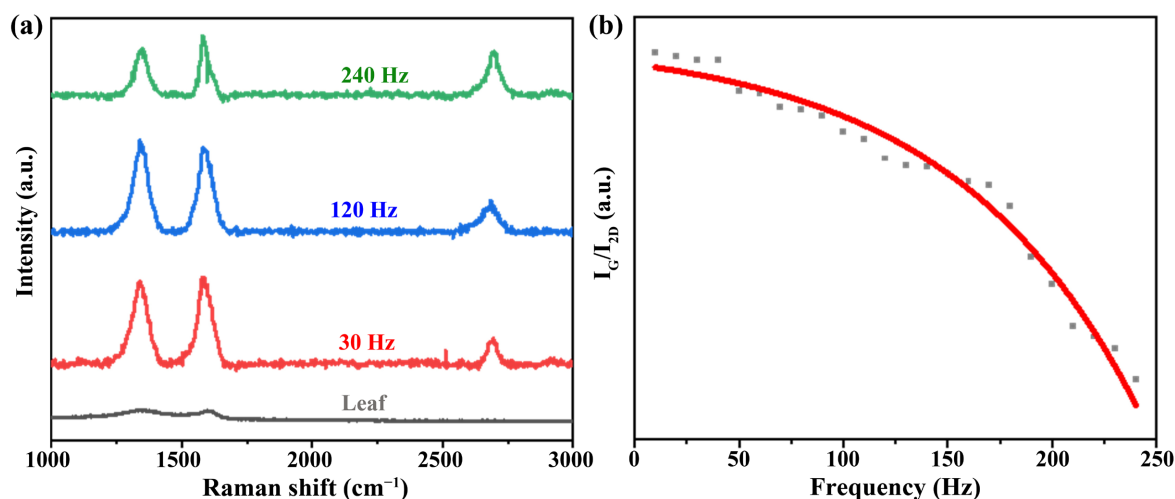


Figure 4. Raman spectra of the products at different frequencies and the variation of I_G/I_{2D} : (a) Raman spectra of the leaf precursor and the products obtained at 30 Hz, 120 Hz, and 240 Hz; (b) Corresponding variation curve of I_G/I_{2D} with pulse frequency
图 4. 不同频率下产物的拉曼光谱及 I_G/I_{2D} 变化情况: (a) 树叶及 30 Hz、120 Hz、240 Hz 下产物的拉曼光谱; (b) 脉冲频率与 I_G/I_{2D} 的对应变化曲线

4. 结论

本研究基于碳热冲击所构建的瞬态非平衡热环境,实现了树叶前驱体向乱层石墨烯的快速转化。冲击功率决定产物的石墨化程度和热损伤水平,并存在最佳功率条件以制得缺陷较少、结构较完整且结晶程度较高的乱层石墨烯。脉冲频率决定产物的层数及堆垛状态,脉冲频率的增大能够减少所得乱层石墨烯的层数。通过冲击功率和脉冲频率的协同优化,可制备出高结晶度、层数较少的乱层石墨烯,为之后的大规模可控制备奠定基础。

基金项目

(1) 国家自然科学基金委员会,青年科学基金项目(C类),52202044,石墨烯/铜摩尔超晶格界面的焦耳热构筑及电学性能调控方法研究;

(2) 苏州市科技局,产业前瞻与关键核心技术,SYC2022018,碳纳米管瞬间超高温加热制备高熵纳米微球研发。

参考文献

- [1] Novoselov, K.S., Geim, A.K., Morozov, S.V., Jiang, D., Zhang, Y., Dubonos, S.V., *et al.* (2004) Electric Field Effect in Atomically Thin Carbon Films. *Science*, **306**, 666-669. <https://doi.org/10.1126/science.1102896>
- [2] Geim, A.K. and Novoselov, K.S. (2007) The Rise of Graphene. *Nature Materials*, **6**, 183-191. <https://doi.org/10.1038/nmat1849>

- [3] Novoselov, K.S., Jiang, D., Schedin, F., Booth, T.J., Khotkevich, V.V., Morozov, S.V., *et al.* (2005) Two-Dimensional Atomic Crystals. *Proceedings of the National Academy of Sciences*, **102**, 10451-10453. <https://doi.org/10.1073/pnas.0502848102>
- [4] Castro Neto, A.H., Guinea, F., Peres, N.M.R., Novoselov, K.S. and Geim, A.K. (2009) The Electronic Properties of Graphene. *Reviews of Modern Physics*, **81**, 109-162. <https://doi.org/10.1103/revmodphys.81.109>
- [5] Ferrari, A.C. and Robertson, J. (2000) Interpretation of Raman Spectra of Disordered and Amorphous Carbon. *Physical Review B*, **61**, 14095-14107. <https://doi.org/10.1103/physrevb.61.14095>
- [6] Zhu, Y., Murali, S., Cai, W., Li, X., Suk, J.W., Potts, J.R., *et al.* (2010) Graphene and Graphene Oxide: Synthesis, Properties, and Applications. *Advanced Materials*, **22**, 3906-3924. <https://doi.org/10.1002/adma.201001068>
- [7] Stankovich, S., Dikin, D.A., Dommett, G.H.B., Kohlhaas, K.M., Zimney, E.J., Stach, E.A., *et al.* (2006) Graphene-Based Composite Materials. *Nature*, **442**, 282-286. <https://doi.org/10.1038/nature04969>
- [8] Chen, D., Tang, L. and Li, J. (2010) Graphene-Based Materials in Electrochemistry. *Chemical Society Reviews*, **39**, 3157-3180. <https://doi.org/10.1039/b923596e>
- [9] Li, X., Cai, W., An, J., Kim, S., Nah, J., Yang, D., *et al.* (2009) Large-Area Synthesis of High-Quality and Uniform Graphene Films on Copper Foils. *Science*, **324**, 1312-1314. <https://doi.org/10.1126/science.1171245>
- [10] Hummers, W.S. and Offeman, R.E. (1958) Preparation of Graphitic Oxide. *Journal of the American Chemical Society*, **80**, Article No. 1339. <https://doi.org/10.1021/ja01539a017>
- [11] Prekodravac, J.R., Kepić, D.P., Colmenares, J.C., Giannakoudakis, D.A. and Jovanović, S.P. (2021) A Comprehensive Review on Selected Graphene Synthesis Methods: From Electrochemical Exfoliation through Rapid Thermal Annealing Towards Biomass Pyrolysis. *Journal of Materials Chemistry C*, **9**, 6722-6748. <https://doi.org/10.1039/d1tc01316c>
- [12] Seitzhanova, M., Kudyarova, Z., Rakhimova, B., Tugelbayeva, L. and Tauanov, Z. (2025) Synthesis of Biomass-Derived Graphene Nanomaterials by Chemical Activation with KOH. *International Journal of Molecular Sciences*, **26**, Article No. 11255. <https://doi.org/10.3390/ijms262311255>
- [13] Dreyer, D.R., Park, S., Bielawski, C.W. and Ruoff, R.S. (2010) The Chemistry of Graphene Oxide. *Chemical Society Reviews*, **39**, 228-240. <https://doi.org/10.1039/b917103g>
- [14] Eda, G. and Chhowalla, M. (2010) Chemically Derived Graphene Oxide: Towards Large-Area Thin-Film Electronics and Optoelectronics. *Advanced Materials*, **22**, 2392-2415. <https://doi.org/10.1002/adma.200903689>
- [15] Pei, S. and Cheng, H.M. (2012) The Reduction of Graphene Oxide. *Carbon*, **50**, 3210-3228. <https://doi.org/10.1016/j.carbon.2011.11.010>
- [16] Zhu, X., Lin, L., Pang, M., Jia, C., Xia, L., Shi, G., *et al.* (2024) Continuous and Low-Carbon Production of Biomass Flash Graphene. *Nature Communications*, **15**, Article No. 3218. <https://doi.org/10.1038/s41467-024-47603-y>
- [17] Luong, D.X., Bets, K.V., Algozeeb, W.A., Stanford, M.G., Kittrell, C., Chen, W., *et al.* (2020) Gram-Scale Bottom-Up Flash Graphene Synthesis. *Nature*, **577**, 647-651. <https://doi.org/10.1038/s41586-020-1938-0>
- [18] Mahmood, F., Mbeugang, C.F.M., Asghar, F., Xie, X., Lin, D., Liu, D., *et al.* (2025) Understanding the Synthesis of Turbostratic/Flash Graphene via Joule Heating. *Materials*, **18**, Article No. 2892. <https://doi.org/10.3390/ma18122892>
- [19] Zhang, M., Hong, D., Xu, T., Zhang, Y., Sun, M. and Wang, C. (2025) The Graphene Formation via Flash Joule Heating: The Effect of Cooling Rate. *Energy*, **337**, Article No. 138673. <https://doi.org/10.1016/j.energy.2025.138673>
- [20] Xu, M., Deng, B., Wang, T., Ren, Z., Zheng, R., Zhong, J., *et al.* (2026) Ultrafast Flash Joule Heating Upcycles Biogas Residue into High-Quality, Sustainable Graphene Composite Materials. *One Earth*, **9**, Article ID: 101557. <https://doi.org/10.1016/j.oneear.2025.101557>
- [21] Wu, D., Sheng, J., Lu, H., Li, S. and Li, Y. (2025) Mass Production of Graphene Using High-Power Rapid Joule Heating Method. *Chemical Engineering Journal*, **505**, Article ID: 159725. <https://doi.org/10.1016/j.cej.2025.159725>
- [22] Wang, F., Huang, R., Yu, Y., Tan, S., Yuan, R., Yin, J., *et al.* (2026) Sustainable Production of Microalgae-Derived Turbostratic Graphene via Flash Joule Heating. *Bioresource Technology*, **442**, Article ID: 133729. <https://doi.org/10.1016/j.biortech.2025.133729>
- [23] Tan, Z., Mahmood, F., Tian, M., Li, Y., Zhang, Q., Ma, Z., *et al.* (2025) Review of Flash Joule Heating for the Synthesis of Graphene and Other Functional Carbon Materials. *Carbon Energy*, **8**, e70119. <https://doi.org/10.1002/cey2.70119>
- [24] Sevilla, M. and Fuertes, A.B. (2011) Sustainable Porous Carbons with a Superior Performance for CO₂ Capture. *Energy & Environmental Science*, **4**, 1765-1771. <https://doi.org/10.1039/c0ee00784f>
- [25] Chen, X., Bo, X., Ren, W., Chen, S. and Zhao, C. (2019) Microwave-Assisted Shock Synthesis of Diverse Ultrathin Graphene-Derived Materials. *Materials Chemistry Frontiers*, **3**, 1433-1439. <https://doi.org/10.1039/c9qm00113a>
- [26] Barbhuiya, N.H., Kumar, A., Singh, A., Chandel, M.K., Arnusch, C.J., Tour, J.M., *et al.* (2021) The Future of Flash Graphene for the Sustainable Management of Solid Waste. *ACS Nano*, **15**, 15461-15470. <https://doi.org/10.1021/acsnano.1c07571>

- [27] Babel, K. (2004) Porous Structure Evolution of Cellulose Carbon Fibres during Heating in the Initial Activation Stage. *Fuel Processing Technology*, **85**, 75-89. [https://doi.org/10.1016/s0378-3820\(03\)00109-7](https://doi.org/10.1016/s0378-3820(03)00109-7)
- [28] McAllister, M.J., Li, J.L., Adamson, D.H., Schniepp, H.C., Abdala, A.A., Liu, J., *et al.* (2007) Single Sheet Functionalized Graphene by Oxidation and Thermal Expansion of Graphite. *Chemistry of Materials*, **19**, 4396-4404. <https://doi.org/10.1021/cm0630800>
- [29] Gambhir, S., Jalili, R., Officer, D.L. and Wallace, G.G. (2015) Chemically Converted Graphene: Scalable Chemistries to Enable Processing and Fabrication. *NPG Asia Materials*, **7**, e186. <https://doi.org/10.1038/am.2015.47>